Journal of Chromatography, 607 (1992) 69–77
Elsevier Science Publishers B.V., Amsterdam

CHROM. 24 286

Direct measurement of the inverse secondary isotope effects of Rh(I)–C_2H_4 and Rh(I)–C_2H_3D utilizing gas chromatography

Dae Young Youn, Kwang Bum Hong and Kyung-Hoon Jung

Centre for Molecular Science and Department of Chemistry, Korea Advanced Institute of Science and Technology, Taedok Science Town, Taejon 305-701 (South Korea)

Dongho Kim

Spectroscopy and Color Laboratory, Korea Standard Research Institute, Taedok Science Town, Taejon 305-606 (South Korea)

Kyoung-Rae Kim

College of Pharmacy, Sungkyunkwan University, Suwon 440-746 (South Korea)

(First received January 8th, 1992; revised manuscript received April 24th, 1992)

ABSTRACT

The inverse secondary equilibrium isotope effects of Rh(I)–C_2H_4 and Rh(I)–C_2H_3D were directly measured using a gas chromatographic column of dicarbonyl-rhodium(I)-3-trifluoroacetyl-1*R*-camphorate in squalane solution at 283–333 K. Statistical isotope effects were also obtained from a reduced partition function using harmonic vibrational frequencies of RHC–C_2H_4 complexes and normal-mode analysis. The observed isotope effects were in good agreement with those deduced from the reduced partition function. Thermodynamic data of the inverse isotope effect were $\Delta_{D,H}\Delta H = -469 \pm 12$ J mol^{-1} and $\Delta_{D,H}\Delta S = -0.975 \pm 0.017$ J mol^{-1} K^{-1}, where $\Delta_{D,H}\Delta H = \Delta H_D - \Delta H_H$ = the difference of the enthalpy changes of the deuterated and non-deuterated compounds (see refs. 1 and 22) and $\Delta_{D,H}\Delta S = \Delta S_D - \Delta S_H$ = the difference of the entropy changes of the deuterated and non-deuterated compounds. The detailed analysis of the force constant most affected, $F_{C-C} = 8.39$ mdyn/Å, by metal complexation was closer to that of the carbon–carbon double bond (9.1 mdyn/Å) than to that of the carbon–carbon single bond (4.3 mdyn/Å).

INTRODUCTION

The selective separation of olefin isomers by complexation gas chromatography (GC) [1], involving a π-coordination equilibrium complex of metal with substrates (solute), was demonstrated by Bradford *et al.* [2], and extension of its usage for the separation of enantiomers [1,3], and constitutional [4–6] and isotopic isomers has also been reported.

The application of the technique to isotopic ethylene isomers, $C_2H_{4-n}D_n$, has been tested extensively using stationary systems such as silver nitrate–ethylene glycol [7,8], silver nitrate–water [9] and dicarbonyl-rhodium(I)-β-ketoenolates–squalane [1]. In conventional gas–liquid chromatography (GLC), the elution of isotopic samples usually occurs in order of decreasing volatility [10–12], but the order of elution in complexation GC is reversed [1,7–9]. Since this anomaly results from a large inverse

---

Correspondence to: Dr. K.-H. Jung, Centre for Molecular Science and Department of Chemistry, Korea Advanced Institute of Science and Technology, Taedok Science Town, Taejon 305-701, South Korea.

0021-9673/92/$05.00

secondary equilibrium isotope effect between complexes, we considered it a logical extension to measure this anomaly using GC and to correlate it with the inverse isotope effects, K_D/K_H, of metal–olefin complexes, where K_D and K_H are the equilibrium constants of the deuterated and non-deuterated systems, respectively [1,13,14]. It is also worth noting that some of existing data are rather inadequate to correlate the anomaly with the equilibrium phenomena owing to a lack of information regarding the structural properties of the equilibrium complexes.

In this paper we report on the inverse secondary isotope effects of Rh(I)–C_2H_4 and Rh(I)–C_2H_3D determined from the retention data obtained by GC and on the correlation of the measured values with the structural properties of equilibrium complexes obtained from their vibrational characteristics. Differences in the separation factors of Rh(I) and Ag(I) complexes are also correlated in terms of rehybridization of C_2H_4 for metal complexation in conjunction with our previous studies [14].

EXPERIMENTAL

Materials

Ethylene (Matheson), ethylene-d_1 (Merck Sharpe and Dohme, Canada) and methane (Matheson) were used after several freeze–pump–thaw cycles at liquid nitrogen temperature until traceable impurities were no longer detected by GC. For ethylene-d_1 no isotopic purification was attempted. Dicarbonyl-rhodium(I)-3-trifluoroacetyl-1*R*-camphorate (RHC) was purchased from Johnson Matthey.

Gas chromatography

An HP 5880A gas chromatograph equipped with two flame ionization detectors was used to measure K_D/K_H. Sample injection was done using a 1.0-ml internal loop six-port gas sampling valve (Valco) attached to a high-vacuum sampling system line. The GC oven temperature was maintained at the operating temperature of 283–333 K to within ± 0.1 K by a built-in liquid nitrogen cryogenic system.

The separation column for isotopic samples was a 30 m × 2 mm I.D. PTFE column packed with 60–80 mesh Chromosorb P AW DMCS coated with squalane containing 0.06 *M* RHC. The newly prepared column was conditioned by passing helium through at a low flow-rate (*ca.* 5 ml/min) for more than 3 days at room temperature. The freshly made column lasted more than 3 months with minimum change in its activity by preventing unnecessary exposure to air, water or organics.

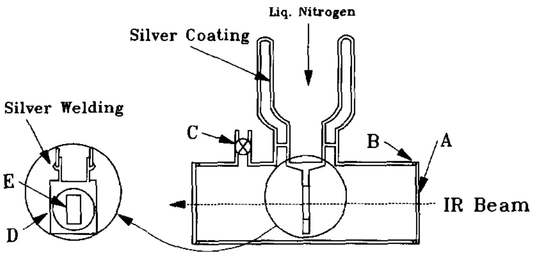

Fig. 1. Low-temperature IR cell for the measurements of solid–gas and liquid–gas interface phenomena. A = window; B = O-ring; C = stopcock; D = copper tip; and E = KBr pellet.

Infrared spectroscopy

Infrared spectra of Rh(I)–olefin complexes were obtained using a Bomen MB 100 spectrometer (Fourier transform infrared FT-IR). Since RHC–olefin complex formation processes are known to be fast reversible reactions, a low-temperature IR cell was used to obtain IR spectra of the equilibrium π-complexes. The IR cell was composed of a 10-cm gas cell with KRS-5 windows (Yanus), 36 mm diameter and 5 mm thickness, at both ends and a copper tip located in the middle of the cell which intersected the IR beam path perpendicularly. A detailed configuration is shown in Fig. 1. The tip had a circular hole in the middle to hold a KBr pellet containing stationary phase in order to form an equilibrium chemical complex with its environment gas, *i.e.* olefins at liquid nitrogen temperature. The potassium bromide/squalane ratio of the pellet was 20:1 and it was mounted on the copper tip using Torr-Seal (Varian). On top of the cell a liquid nitrogen Dewar was attached to chill the pellet through the copper tip heat-transmitting medium. An external blow fan was installed near the cell to prevent deposition of water vapour on the window surface.

Experimental procedures

Gas chromatographic and IR spectroscopic measurements in conjunction with the normal-mode analyses were made to obtain the equilibrium and statistical isotope effects, respectively.

The equilibrium isotope effect was obtained from retention data of both C_2H_4 and C_2H_3D in an RHC–squalane stationary phase system. The retention data were observed by injecting a sample mixture of C_2H_4–C_2H_3D–CH_4 (10:10:1) into the gas chromatograph at a flow-rate of 14.6 ml/min at 283–333 K. Sample pressures for GC injection were kept at <1 Torr to prevent column overloading, which causes lowering of retention time and peak tailing [15]. Methane gas was used as an internal reference to measure the dead volume of the instrument and the relative corrected retention volumes of the olefins.

The statistical isotope effect was deduced from the experimentally observed IR spectra and the vibrational frequencies calculated by normal-mode analyses of the olefins and the complex molecules. Since the vibrational frequencies of both olefins have been well studied [16–18], the normal-mode analyses of these compounds, checked against the literature values, were utilized to obtain transfer force constants for the analysis of the complex molecules. However, the vibrational frequencies of RHC–olefin equilibrium complexes have not been available up until now. We have obtained IR spectra of the complexes using the low-temperature IR cell and performed the analysis utilizing our calculated force constants as well as literature values [19] for similar compounds such as $[RhCl(C_2H_4)_2]_2$ or $[RhBr(C_2H_4)_2]_2$. To obtain IR spectra, gas samples were introduced into the gas cell, prechilled with liquid nitrogen and evacuated. The temperature of the tip or pellet was not monitored but was assumed to be that of liquid nitrogen since the system was continuously pumped and cooled long enough for it to reach equilibrium temperature with the cooling system. The sample pressure was varied to obtain the best IR spectrum. These pressures were *ca.* 1 atm at liquid nitrogen temperature owing to condensation of samples around the upper part of the tip but they were *ca.* 20 Torr at room temperature where condensation did not occur. To accomplish complete normal-mode analysis of the complexes, one should have complete knowledge of the geometrical structures of the complexes. However, since the structures of neither RHC nor RHC–olefins are well known [20], we have treated the complexes as free Rh–olefin complex molecules for the calculations. This simplified calculation is further justified by the fact that the interaction between the vicinal group CO, which is covalently bound to Rh, and Rh–olefin is not so prominent and hence the complete calculation is impractical.

The free Rh(I)–olefin spectra were acquired by subtracting the free RHC spectra from the RHC–olefin spectra using the spectra subtraction function, Bomen program. The spectra obtained by subtraction contained high background noise. This noise was eliminated by averaging 10–20 repeated runs of the same spectra.

RESULT AND DISCUSSION

Determination of isotope effect, K_D/K_H, using complexation GC

The retention volumes of C_2H_4 and C_2H_3D were obtained from chromatograms of these compounds by analysing on an RHC–squalane stationary phase. The retention volumes were expressed as a product of the partition equilibrium between the gas phase and the liquid phase of the olefin of interest, and the thermodynamic association equilibrium between the olefin and the metal complex [21]. The expression can be approximated with an equilibrium constant (K_H or K_D) when the relative corrected retention volume of the olefin with respect to methane as an inert reference standard on RHC–squalane (r_H or r_D) is larger than that on pure squalane ($r_{\circ H}$ or $r_{\circ D}$). Consequently, the inverse secondary isotope effect, K_D/K_H, is reduced to [1]:

$$K_D/K_H \approx (r_D/r_H) \times (r_{\circ H}/r_{\circ D}) \qquad (1)$$

where r_D/r_H and $r_{\circ H}/r_{\circ D}$ are the relative corrected retention volume ratios or the separation factor on RHC–squalane and on pure squalane, respectively, using methane as an inert reference material. r_D/r_H is directly measured from the retention data, while the direct measurement of $r_{\circ H}/r_{\circ D}$ is impractical since it requires a long squalane column causing peak broadening too large to handle. Alternatively, $r_{\circ H}/r_{\circ D}$ can be obtained from the relationship $r_{\circ H}/r_{\circ D} \approx P_D/P_H$, where P_D and P_H are the vapour pressures of deuterated and non-deuterated solutes on an apolar stationary phase, respectively [22]; the ratio of retention volumes is inversely proportional to that of the vapour pressures of constituents on an apolar

TABLE I

GAS CHROMATOGRAPHIC PROPERTIES OF ETHYLENE AND ETHYLENE-D_1 ON THE RHC–SQUALANE STATIONARY SYSTEM

Temperature (K)	K_D/K_H	r_D/r_H	$r^{\circ}_{H}/r^{\circ}_{D}$ [a]
283	1.087	1.078	1.0080
293	1.076	1.068	1.0079
303	1.070	1.062	1.0078
313	1.065	1.057	1.0077
323	1.060	1.052	1.0076
333	1.053	1.045	1.0074

[a] $r^{\circ}_{H}/r^{\circ}_{D}$ is calculated from the relationship $r^{\circ}_{H}/r^{\circ}_{D} \approx P_D/P_H$ and $\ln(P_H/P_D) = 406/T^2 - 3.687/T$ [23].

stationary phase and can be expressed by a simple empirical relationship [23]. The deduced inverse secondary isotope effects, the ratios of relative corrected retention volume on both RHC-squalane and neat squalane at a set of temperatures, are listed in Table I. A typical chromatogram is displayed in Fig. 2. The separation factors measured on the 30-m packed column used for this study were approximately the same as those on a 200-m stainless-steel capillary column in the literature [1]. Average thermodynamic values deduced from the partition equilibrium secondary isotope effects $\Delta_{D,H}\Delta H$ and $\Delta_{D,H}\Delta S$, obtained at different temperatures, by Gibbs–Helmholz plot are -469 ± 12 J mol^{-1} and -0.975 ± 0.017 J mol^{-1} K^{-1}, respectively, where $\Delta_{D,H}\Delta H = \Delta H_D - \Delta H_H$ = the difference of the enthalpy changes of the deuterated and non-deuterated compounds (see refs. 1 and 22) and $\Delta_{D,H}\Delta S = \Delta S_D - \Delta S_H$ = the difference of the entropy changes of the deuterated and non-deuterated compounds.

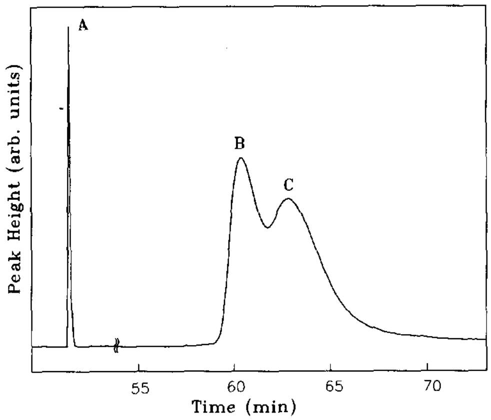

Fig. 2. Typical chromatogram of C_2H_4 and C_2H_3D on an RHC–squalane stationary phase system. GC conditions: oven temperature, 323 K; carrier gas flow-rate, 14.6 ml/min. A, B and C refer to internal standard CH_4 (retention time = 13.0 min), C_2H_4 (60.5 min) and C_2H_3D (63.1 min), respectively.

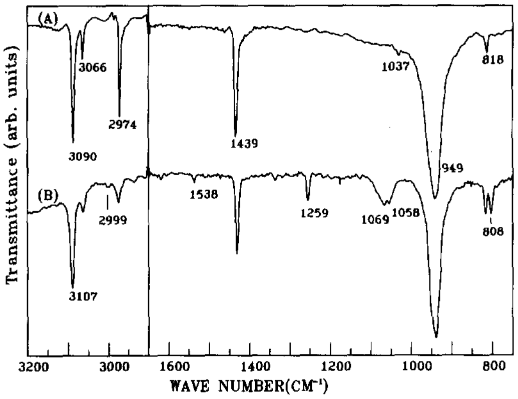

Fig. 3. IR spectra of free ethylene (A) and the ethylene portion in of the RHC–C_2H_4 complex (B).

The bonding structures of metal–olefin π-complexes can be explained well by the two-way donor–acceptor model known as the Dewar–Chatt–Duncanson model [24,25], in which the bondings are composed of a dative σ-bond [π(olefin) → metal] and a π-back-bond [metal → π*(olefin)]. The quantitative contributions of the two bonds in Ag(I)–C_2H_4 and in Rh(I)–C_2H_4 complexes are not well understood, but the dative σ-bond is known to be relatively more dominant than the π-back-bond for both complexes [1,26,27]. Consequently, one would expect the more electronegative Rh(I) to form a stronger Rh(I)–C_2H_4 bond than Ag(I)–C_2H_4 and hence the separation factor on an Rh(I) column to be larger than that on an Ag(I) column. These phenomena are supported by our observed secondary isotope effect for Rh(I), *e.g.* 1.087 on RHC–squalane at 283 K is larger than 1.047 on silver nitrate–ethylene glycol at 273 K [14].

Infrared spectroscopic studies

An IR spectroscopic study was undertaken to determine the vibrational characteristics of Rh(I)–C_2H_4 and the structural changes occurring during the complexation. The ethylene portion of the spectrum was obtained by subtracting the free RHC spectrum from that of RHC–C_2H_4. By scanning the RHC–squalane solution at liquid nitrogen temperature, we obtained shifted ethylene bands in the ethylene portion of the spectrum (shown in Fig. 3) together with the band of free C_2H_4 adsorbed on KBr surface, which we compared with that obtained at room temperature and that of the RHC–C_2H_4–KBr pellet. The observed frequencies of free C_2H_4 are similar to those of a thick film (a few microns) of C_2H_4 obtained by Dows [28] at 65 K. The ethylene portion of the spectra demonstrated two types of spectra, *i.e.* one composed of uncomplexed C_2H_4 bands and the other composed of shifted bands caused by complexation. The uncomplexed C_2H_4 bands in the scan showed less than $\pm 2\ \mathrm{cm}^{-1}$ shift of line frequencies except for 3107 cm^{-1}. The large shift for the 3107 cm^{-1} band, *ca.* 17 cm^{-1}, is interpreted as a cause of the convolution of the 3090 cm^{-1} free C_2H_4 band and the hidden complexed band around 3107 cm^{-1}. In the C_2H_4 portion of the spectrum, we could identify seven frequencies among fifteen fundamental frequencies of Rh(I)–C_2H_4 complex ranging from 400 to 4000 cm^{-1}. In the 1650–750 cm^{-1} range, like other transition metal complexes [29–31], we also observed several relatively high-intensity peaks. The 1538 and 1259 cm^{-1} peaks are assigned to C=C stretching and CH_2 in-phase scissoring motion, respectively, by reference to other metal complexes. These bands play key roles in predicting the degree of C=C bond rehybridization on metal–olefin complexes [29–32]. Stuve and Madix [32] proposed the $\pi\sigma$-parameter as a measure of the degree of C_2H_4 rehybridization in adsorption. This parameter takes into account the vibrational coupling of these two bands and ranges from 0 to 1, *i.e.* 0 for gaseous C_2H_4, 0.38 for Zeise's salt, a model for π-bonded C_2H_4 and 1 for $C_2H_4Br_2$, a model for di-σ-bonded C_2H_4. The calculated $\pi\sigma$-parameter of Rh(I)–C_2H_4, 0.31, obtained from 1538 and 1259 cm^{-1}, is larger than that of Ag(I)–C_2H_4, 0.12, obtained from 1579 and 1320 cm^{-1} bands [33] of $[Ag(C_2H_4)]BF_4$. Since C_2H_4 in Rh(I)–C_2H_4 is rehybridized more than that in Ag(I)–C_2H_4, one would expect the separation factor to be larger in an Rh(I) column than in an Ag(I) column. Though the simplified calculation given above predicts the $\pi\sigma$-parameters reasonably well, it requires further information on coupling parameters such as the geometry, the magnitude of force constants and the degree of coupling between each mode for more precise calculation. These are discussed in some detail in the normal-mode analysis section.

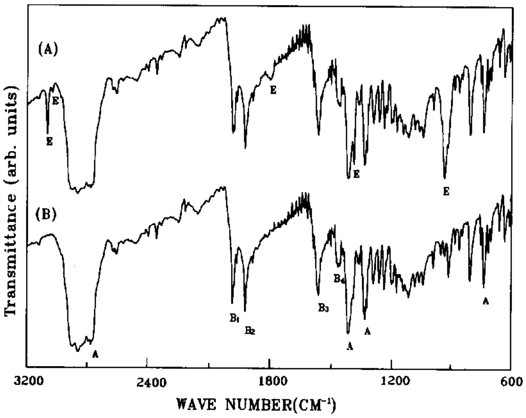

Fig. 4. IR peak assignments for RHC–C_2H_4 peaks (A) and neat RHC peaks (B). The letters A, B_1, B_2, B_3, B_4 and E on both IR spectra refer to squalane, C≡O asymmetric stretching, C≡O symmetric stretching, C=O asymmetric stretching, C=O symmetric stretching and ethylene peaks, respectively.

Both 1069 and 1058 cm^{-1} bands can be assigned as either dimer bands or CH_2 wagging bands (A_1 and B_1) because of their broad nature [28]. We assigned these bands to the waggings on the experimental ground that stoichiometrically different species other than the 1:1 complex were not found during all our observations and the shift to higher frequencies agrees with the generally increasing trend of the wagging frequency by complexation [31]. The 808 cm^{-1} band is assigned to CH_2 bending mode shifted from 819 cm^{-1} of free C_2H_4. Though our observed weak band at 2999 cm^{-1} and a hidden band around 3107 cm^{-1} are well within the 3200–2900 cm^{-1} range of the CH stretching region, CH stretching motions attributed to Rh(I)–C_2H_4 are difficult to assign on the basis of IR spectra alone because of their weak absorption and strong tendency to overlap free C_2H_4 bands. These are, therefore, assigned to CH stretching bands with less confidence.

Fig. 4 displays the strong characteristic peaks at 2089, 2021, 1628 and 1519 cm^{-1} in full spectra of RHC and RHC–C_2H_4. The first two bands are assigned to C≡O asymmetric and symmetric stretchings, and the last two are C=O asymmetric and symmetric stretchings. The observation of frequency

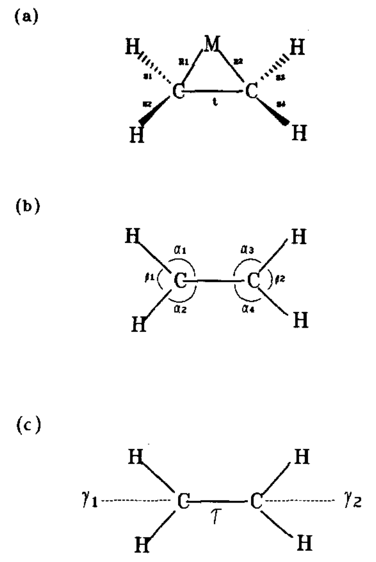

Fig. 5. Internal coordinate assignments for Rh(I)–C_2H_4 complex. (a) The stretching coordinates; (b) the bending coordinates; and (c) the wagging and torsional coordinates. Adapted from ref. 16.

shift of these bands from RHC to RHC–C_2H_4 may give a good idea of structural changes in the RHC skeleton. Schurig and Gil-Av [20] have proposed that the square planar shape of uncomplexed RHC is changed to trigonal bipyramid by olefin complexation with the CO groups in apical, and the olefin and β-diketonate in equatorial, positions. In our system, however, no considerable band shifts were observed from RHC to RHC–C_2H_4, and these findings indicate that there are very few structural changes between the four coordinates of RHC and the intermediate five coordinates of RHC–C_2H_4. Consequently, we suggest that the structure of the intermediate five coordinates of RHC–C_2H_4 complexes is closer to the square pyramid geometry. It is also likely that there is no structural change in RHC during the reaction with C_2H_4 since the IR spectra of both fresh RHC and used RHC are almost identical.

Normal-mode analysis

Normal-mode analysis was used to compare quantitatively the molecular parameters of the Rh(I)–C_2H_4 complex and those of other π-complexes and to assign vibrational frequencies of Rh(I)–C_2H_3D. We used valence force fields [34] obtained from the seven observed frequencies of the C_2H_4 portion of the spectrum of the RHC–C_2H_4 complex and its assumed geometry. The geometries of the complexes are assumed on the basis of X-ray data of Rh-containing compounds [35,36], and these are Rh(I)–C = 2.2, C–C = 1.38, C–H = 1.09 Å and <HCH = 120°, with the C_2H_4 group held in a planar structure as shown in Fig. 5. For the choice of internal coordinates, a factor to bear in mind was facilitation of the quantitative comparison with other metal–ethylene complexes within the same framework [29,30,37]. The calculations and discussions are emphasized, in particular the coupling parameters, which are responsible for the degree of C_2H_4 rehybridization of metal–C_2H_4 complexes in complexation GC, and vibrational frequencies re-

TABLE II

CALCULATED FUNDAMENTAL FREQUENCIES OF Rh(I)–C_2H_4 AND Rh(I)–C_2H_3D AND THE OBSERVED VALUES OF THE ETHYLENE PORTION IN THE SPECTRUM OF RHC–C_2H_4 COMPLEX

F_{Rh-C} = 1.13 mdyn/Å, F_{C-C} = 8.39 mdyn/Å, F_{C-H} = 5.09 mdyn/Å, $F_{<CCH}$ = 0.54 mdyn Å, $F_{<CCH,<CCH}$ = −0.01 mdyn Å, $F_{<HCH}$ = 0.39 mdyn Å, $F_{<HCH,<HCH}$ = 0.07 mdyn Å, F_{wag} = 0.186 mdyn Å, $F_{wag,wag}$ = 0.06 mdyn Å, F_{twist} = 0.175 mdyn Å and $F_{C-C,<HCH}$ = −0.375 mdyn.

Mode characteristics	Observed value	Calculated value	
		Rh(I)–C_2H_4	Rh(I)–C_2H_3D
A_1			
ν_1: CH stretch		3010	2263
ν_2: C=C stretch	1539	1538	1517
ν_3: CH_2 scissor	1259	1259	1231
ν_4: CH_2 wag	1058	1058	913
ν_5: Rh–C stretch		393	388
A_2			
ν_6: CH stretch		3121	3115
ν_7: CH_2 rock		1212	1089
ν_8: CH_2 twist		1150	1122
B_1			
ν_9: CH stretch	2999	2991	3001
ν_{10}: CH_2 scissor		1423	1371
ν_{11}: CH_2 wag	1069	1068	1063
ν_{12}: Rh–C stretch		324	311
B_2			
ν_{13}: CH stretch	3107	3107	3063
ν_{14}: CH_2 rock	808	809	714

$$K_D/K_H = \frac{(s_1/s'_1)\prod_i (U'_{1i}/U_{1i})\exp[(U_{1i} - U'_{1i})/2][1 - \exp(-U_{1i})/1 - \exp(-U'_{1i})]}{(s_2/s'_2)\prod_i (U'_{2i}/U_{2i})\exp[(U_{2i} - U'_{2i})/2][1 - \exp(-U_{2i})/1 - \exp(-U'_{2i})]} \tag{2}$$

sponsible for the inverse secondary isotope effect. The present model includes fourteen out of fifteen vibrations for Rh(I)–C_2H_4 and does not take into account a B_1 tilting motion, since it is expected to have a very low frequency and hence very small isotopic shift [29,30]. Two Rh–C stretching modes, causing relatively large isotopic shifts, were obtained from the normal-mode analysis, and these are 393 and 324 cm^{-1}. For the calculation, we used a transferred force constant, F_{Rh-C} = 1.13 mdyn/Å from similar systems. The transferred force constant was deduced from known Rh–C stretching frequencies of other Rh-containing molecules such as 399 cm^{-1} in $[RhCl(C_2H_4)_2]_2$ [19], 393 cm^{-1} in $[RhBr(C_2H_4)_2]_2$ [19], 355 cm^{-1} in adsorbed C_2H_4 on Rh(111) [31] and two peaks at 325 and 395 cm^{-1} in adsorbed C_2H_4 on Rh(100) [31]. The same geometrical parameters and force constants were assumed for Rh(I)–C_2H_3D). The observed and calculated frequencies are listed in Table II for both Rh(I)–C_2H_4 and Rh(I)–C_2H_3D.

For general trends of metal–olefin complexes, Bent *et al.* [31] have suggested a method of predicting the correlation of the degree of the rehybridization with the mode frequencies of C_2H_4. The trends are that the CC and CH stretching and CH_2 bending mode frequencies are decreased but the wagging and twisting are increased by complexation. For all calculation force constant F_{C-C} is clearly the most affected by metal complexation. Compared with free C_2H_4 F_{C-C} is reduced from 9.1 to 8.39 mdyn/Å and found to be closer to that of a double bond than to that of a single bond, 4.3 mdyn/Å [29,30], in cyclopropane. Comparative studies with other metal complexes were also made. These are 6.14 mdyn/Å [37] for $(C_2H_4)Fe(CO)_4$ and 4.23 mdyn/Å [37] for $K[PtCl_3(C_2H_4)]H_2O$, which suggest CC single-bond characters in both Fe and Pt complexes, while the 8.91 mdyn/Å value for $[Ag(C_2H_4)]BF_3$ is quite similar to that of RHC–C_2H_4 and CC double-bond character. The reduction in F_{C-C} represents a higher degree of rehybridization of C_2H_4 in metal complexes. Both Ag(I)–C_2H_4 and Rh(I)–C_2H_4 show double-bond character, form reversible equilibrium complexes and can be used as stationary phases in complexation GC, whereas both Fe–C_2H_4 and Pt–C_2H_4, show single-bond character and form the stable complexes at room temperature. From the foregoing discussion, we conclude that the degree of rehybridization of C_2H_4 in metal complexes is greatly affected by the chemical and physical properties of the metal–olefin complex. The higher separation factor in Rh(I) than in Ag(I) columns is also responsible for the higher degree of rehybridization of C_2H_4 in Rh(I)–C_2H_4 than in Ag(I)–C_2H_4.

Statistical isotope effect

The statistical inverse secondary isotope effect was calculated from the reduced partition functions, expressed in terms of the normal–mode vibrations of the molecules involved. It can be expressed in terms of the reduced partition function, $(s/s')f$, the ratio of the uncomplexed and the complexed molecules, *i.e.* $(s_1/s'_1)f[C_2H_3D/C_2H_4]/(s_2/s'_2)f[Rh(I)–C_2H_3D/Rh(I)–C_2H_4]$. A more comprehensive expression using the complete set of normal-mode frequencies, v_i, is as in eqn. 2 [38,39], where subscripts 1 and 2 represent the complex and free C_2H_4, respectively. The primed quantities refer to the deuterated molecules. U_i has its usual meaning, hv_i/kT. The symmetry number, s, for C_2H_4, C_2H_3D, Rh(I)–C_2H_4 and Rh(I)–C_2H_3D is 4, 2, 2 and 1, respectively. For simplicity, eqn. 2 can be resolved into three terms:

$$K_D/K_H = (VP)(ZPE)(EXC) \tag{3}$$

where $VP = (s_1/s'_1)\prod_i (U'_{1i}/U_{1i})/(s_2/s'_2)\prod_i (U'_{2i}/U_{2i})$,

$ZPE = \prod_i \exp[(U_{1i} - U'_{1i})/2]/\prod_i \exp[(U_{2i} - U'_{2i})/2]$

and $EXC = \prod_i[1 - \exp(-U_{1i})/1 - \exp(-U'_{1i})]/$

$\prod_i [1 - \exp(-U_{2i})/1 - \exp(-U'_{2i})]$ and where VP, ZPE and EXC represent the vibrational product, the zero-point energy and the vibrational excitation

TABLE III

CALCULATED AND OBSERVED VALUES OF K_D/K_H AND VP, ZPE, AND EXC TERMS AS A FUNCTION OF TEMPERATURE

Temperature (K)	K_D/K_H[a]	VP	ZPE	EXC
283	1.086 (1.087)	0.921	1.158	1.018
293	1.078 (1.076)	0.921	1.148	1.019
303	1.070 (1.070)	0.921	1.140	1.019
313	1.064 (1.065)	0.921	1.133	1.020
323	1.059 (1.060)	0.921	1.127	1.020
333	1.054 (1.053)	0.921	1.121	1.021

[a] The observed values in the RHC–squalane column are in parentheses.

terms, respectively. The VP term comes from the classical translational and rotation partition function, given by the Redlich–Teller product rule for the isotopically substituted compounds. The ZPE and EXC terms are from the classical vibrational partition function. The calculated values of K_D/K_H at different temperatures together with the observed values are shown in Table III. The calculated $\Delta_{\mathrm{D,H}}\Delta H$ and $\Delta_{\mathrm{D,H}}\Delta S$ values are -469 J mol^{-1} and -0.975 J mol^{-1} K^{-1}, respectively. The calculated values are in good agreement with those obtained experimentally by GC. Investigation of the data in Table III reveals several interesting points. The positive contributions are mainly attributable to the ZPE and EXC terms, whereas the negative contribution comes from the VP term. The temperature dependence of each term also shows some interesting phenomena. The VP term is temperature-independent and the slight positive effect of EXC cancels the negative dependency of ZPE; thus, the overall effect shows little temperature dependency.

CONCLUSIONS

In this paper we report on the successful achievement of a method to correlate the equilibrium isotope effect with the statistical isotope effect of Rh(I)–C_2H_4 and Rh(I)–C_2H_3D. The equilibrium isotope effect is directly measured by the GC technique using RHC–squalane as the stationary phase. The statistical isotope effect is deduced from the reduced partition function based on the RHC–C_2H_4 vibrational frequencies acquired from IR spectroscopic data. The larger separation factor of Rh(I)–olefins compared with that of Ag(I)–olefins is caused by their greater rehybridization capabilities. Both the $\pi\sigma$-parameter and F_{C-C} are useful to the degree of rehybridization of C_2H_4 in metal–olefin complexes, which can be used to predict the physical and chemical properties of metal–olefin complexes. The procedures used in this study provided insight into the physical separation of olefinic isotopes in complexation GC and clarification of the molecular properties of metal–olefin complexes.

ACKNOWLEDGEMENTS

This work was carried out with financial assistance from the Korea Standards Research Institute and the Korea Science and Engineering Foundation, which is gratefully acknowledged.

REFERENCES

1 V. Schurig, *Chromatographia*, 13 (1980) 263 and earlier references therein.
2 B. W. Bradford, D. Harvey and D. E. Chalkley, *J. Inst. Petrol., London*, 41 (1955) 80.
3 V. Schurig, *Angew. Chem., Int. Ed. Engl.*, 16 (1977) 110.
4 E. Gil-Av and V. Schurig, *Anal. Chem.*, 43 (1971) 2030.
5 V. Schurig, R. C. Chang, A. Zlatkis, E. Gil-Av and F. Mikes, *Chromatographia*, 6 (1973) 223.
6 A. M. Soto, N. Yanagihara and T. Ogura, *Anal. Chem.*, 63 (1991) 1178.
7 R. J. Cvetanovic, F. J. Duncan and W. E. Falconer, *Can. J. Chem.*, 41 (1963) 2095.
8 J. G. Atkinson, A. A. Russell and R. S. Stuart, *Can. J. Chem.*, 45 (1967) 1963.
9 S. P. Wasik and W. Tsang, *J. Phys. Chem.*, 74 (1970) 2970.
10 K. E. Wilzbach and P. Riesz, *Science*, 126 (1957) 748.
11 W. E. Falconer and R. J. Cvetanovic, *Anal. Chem.*, 34 (1962) 1064.
12 F. Bruner, P. Ciccioli and A. Di Corcia, *Anal. Chem.*, 44 (1972) 894.
13 R. J. Cvetanovic, F. J. Duncan, W. E. Falconer and R. S. Irwin, *J. Am. Chem. Soc.*, 87 (1965) 1827.
14 K. B. Hong, K.-H. Jung and S. H. Kang, *Bull. Korea Chem. Soc.*, 3 (1982) 79.
15 D. Y. Youn, S. J. Yun and K.-H. Jung, *J. Chromatogr.*, 591 (1992) 19.
16 K. Machida, *J. Chem. Phys.*, 44 (1966) 4186.
17 B. L. Crawford, Jr., J. E. Lancaster and R. G. Inskeep, *J. Chem. Phys.*, 21 (1953) 678.
18 P. Pulay and W. Meyer, *J. Mol. Spectrosc.*, 40 (1971) 59.
19 M. A. Bennett, R. J. H. Clark and D. L. Milner, *Inorg. Chem.*, 6 (1967) 1647.
20 V. Schurig and E. Gil-Av, *Chem. Commun.*, (1971) 650.
21 V. Schurig, R. C. Chang, A. Zlatkis and B. Feibush, *J. Chromatogr.*, 99 (1974) 147.

22 F. Bruner, G. P. Cartoni and A. Liberti, *Anal. Chem.*, 38 (1966) 298.
23 M. J. Stern, W. A. Van Hook and M. Wolfsberg, *J. Chem. Phys.*, 39 (1963) 3179.
24 J. Chatt and L. A. Duncanson, *J. Chem. Soc.*, (1953) 2939.
25 M. J. S. Dewar, *Bull. Soc. Chim. Fr.*, 18 (1951) C79.
26 H. Basch, *J. Chem. Phys.*, 56 (1972) 441.
27 M. J. S. Dewar and G. P. Ford, *J. Am. Chem. Soc.*, 101 (1979) 783.
28 D. A. Dows, *J. Chem. Phys.*, 36 (1962) 2833.
29 L. Manceron and L. Andrews, *J. Phys. Chem.*, 94 (1990) 3513.
30 L. Manceron and L. Andrews, *J. Phys. Chem.*, 93 (1989) 2963.
31 B. E. Bent, C. M. Mate, L.-T. Kao, A. J. Slavin and G. A. Somorjai, *J. Phys. Chem.*, 92 (1988) 4720.
32 E. M. Stuve and R. J. Madix, *J. Phys. Chem.*, 89 (1985) 3183.
33 D. B. Powell, J. G. V. Scott and N. Sheppard, *Spectrochim. Acta*, 28A (1972) 327.
34 E. B. Wilson, Jr., J. C. Decius and P. C. Cross, *Molecular Vibrations*, McGraw-Hill, New York, 1955.
35 M. Herberhold, *Metal π-Complexes*, Vol. 2, Elsevier, Amsterdam, 1974.
36 H. W. Quinn and J. H. Tsai, *Adv. Inorg. Chem. Radiochem.*, 12 (1969) 217.
37 D. C. Andrews, G. Davidson and D. A. Duce, *J. Organometal. Chem.*, 101 (1975) 113.
38 J. Bigeleisen and M. G. Mayer, *J. Chem. Phys.*, 15 (1947) 261.
39 R. F. Hout, Jr., M. Wolfsberg and W. J. Hehre, *J. Am. Chem. Soc.*, 102 (1980) 3296.